CHARACTERISTIC STUDY OF NON-CIRCULAR INCOMPRESSIBLE FREE JET

By

Ponnambalam. MANIVANNAN * and B.T.N. SRIDHAR *

*Associate. Professor, Dept. of Aeronautical Engineering, Hindustan College of Engineering, Chennai, India. *Email: manicadme42@gmail.com*

** Professor, Department of Aerospace Engineering MIT, Anna University, Chennai, India

This paper reports an experimental investigation of bulk properties of turbulent, which is three dimensional, incompressible, air jets issuing into still air surrounding from the nozzles. The jet orifices utilised included circular, hexagonal and cruciform geometries. Experimental results of pertinent mean flow properties such as axis velocity decay, half width growth, potential core and turbulence intensities are reported. Single Hotwire anemometer was used for measurements of the velocity field. The experiment for the three jets was conducted under the same nominal conditions with the exit Reynolds number of 15,400. Consistent with previous investigations of other non circular jets, the cruciform jet is found to have an overall superior mixing capability over the circular counter part. Immediately downstream of the nozzle exit, it entrains, and then mixes with, the surroundings at a higher rate. This jet has a shorter potential core with higher rates of decay and spread than the circular jet. This phenomenon of axis switching is also found to occur in this jet

Keywords*: Noncircular jets, Cruciform, Hexagon, Half width, Turbulence intensity.*

1. Introduction

The detailed research in the noncircular jets has been performed in the past two decades, because largely due to their potential to entrain ambient fluid more effectively than comparable circular jets. The superior mixing capability of such jets is experimentally related either to the non-uniform curvature or their initial parameter, relative to the evenness for the circular configuration, or to the instabilities produced by the initial perimeter's sharp corners through the asymmetric distribution of pressure and mean flow field [7]. Both phenomena are deduced to accelerate three-dimensionality of the jet structures, therefore causing greater entraining and mixing. For elliptic and rectangular jets, azimuthal curvature variation of initial vortical structure produces non-uniform self-induction and three-dimensional structures. As a result, these flows spread more rapidly in the minor axis plane than in the major axis plane. The minor axis was causing axis switching at a certain distance from the nozzle exit [7, 27]. For corner containing configurations, the corners promote the formation

of fine scale mixing [8, 12]. The above experimental results have also been demonstrated in a number of numerical simulations [5, 6, 15]. The review of [7] summarises both experimental and numerical studies in the context of non-circular jets.

The jet entrainment and spreading rates can, in fact, be assessed via the centerline mean velocity decay and the jet half-velocity width profiles [2, 3]. The jet half-velocity width is defined as the distance from the centerline to the radial location [i.e. Y-location] where the mean streamwise velocity becomes half of the centerline velocity. In fact, the centerline mean velocity decay and jet half-velocity width are, indicators of fluid entrainment rate and the level of jet spreading respectively. In a turbulent jet flow, it is customary to use an axisymmetric nozzle, as reported in [11, 14, 26] to mention only a few. The conventional axisymmetric nozzles consist of a smooth circular pipe or a contracted circular nozzle, which are characterized by fully developed velocity profiles, and top-hat velocity profiles, respectively. Xu and Antonia [26] examined both of these nozzles jet flow configurations and observed that there was slight improvement in fluid entrainment and jet spreading rates of the contoured circular nozzle as compared to the fully developed turbulent jet pipe flow.

It was reported that asymmetric nozzles [especially the triangular, rectangular, and elliptical nozzles] promote higher entrainment and jet spreading compared to their circular [axisymmetric] counterparts [9, 10, 13, 17, 18]. Among the studies on asymmetric nozzles [9, 10, 13, 17, 18], it was reported that, for an instance, the triangular nozzle's jet has a higher entrainment rate than the rectangular jet.

The previous investigations on noncircular jets [1-28], have focused, predominantly on elliptical, rectangular [including square], and triangular configurations. Few detailed measurements and simulations have been performed for other shapes. Although Mi et.al. [13] provided hot wire measurements in nine different shaped jets, their data were limited only to the centerline mean and rms of the axial velocity.

Results of fluid entrainment rate indicated by the centerline velocity decay of isosceles and equilateral triangular nozzles as reported by Mi et al.[13] differ from those of Quinn [18]. While Mi et al. [13], who used nine different nozzle geometries, found that their isosceles triangular jet induced a better entrainment rate than its counterpart equilateral triangular jet; Quinn [18] reported the opposite scenario. Furthermore, Zaman [27], and Gutmark and co-workers [9] reported discrepancies concerning the extent of the increase in jet spreading and entrainment of rectangular nozzles as opposed to circular nozzles. Indeed, while Gutmark and co-workers [9] observed considerable increase in jet spreading and entrainment of the rectangular nozzles [with an aspect ratio of 2:1] compared to their circular nozzle counterpart, Zaman [27],

The present study carried out with hotwire anemometer measurements of three single jets issuing respectively from circular, hexagonal and cruciform orifices, and hydraulic diameter of approximately 15mm [fig. 1]. The previous research mainly focus on the different noncircular shapes like ellipse, triangle, square, rectangle etc. all the shapes having 3 or 4 corners only. To study the jet behaviour, when increase the number of corners of the non circular nozzle shapes like hexagon and cruciform and also compare the flow and turbulent characteristics of circular and noncircular jets.

2. Experimental Setup Details

A block diagram of present experimental investigation of jet is shown in fig. 1. It consisted of

a centrifugal blower, jet assembly, and two-dimensional traversing platform. The three nozzles (fig. 2.) were separately attached to the exit pipe of 50mm internal diameter. The flow rate through the pipe, which was used to calculate the jet exit bulk velocity and Reynolds number, was obtained by a flow meter. The previous literatures have shown that initial conditions play a determining role for the mixing of the jet. Special care has been taken in the design of the nozzles. To be able to compare results from the non-circular nozzles to those from the circular nozzles, the non-circular nozzles have been designed to have the same hydraulic diameter as the circular nozzles. The contour of the nozzle is well machined to suppress the boundary layer thickness so that the uniform velocity profile is obtained at the exit of the nozzle. A matched third-degree polynomial with zero first derivative ends has been used to design the nozzle in order to avoid separation on the inner jet surface. The flow meter was attached at a distance of 10 D_h from the nozzle exit. Good axis symmetry of the jet flow immediately upstream of the orifice attached was achieved. Since nearly identical and symmetric radial profiles of the mean velocity at the jet exit for different orientations were found (fig. 3). The axial turbulence was about 3% at the center. All the jets were measured at the same nominal Reynolds number of Re = 15,400.

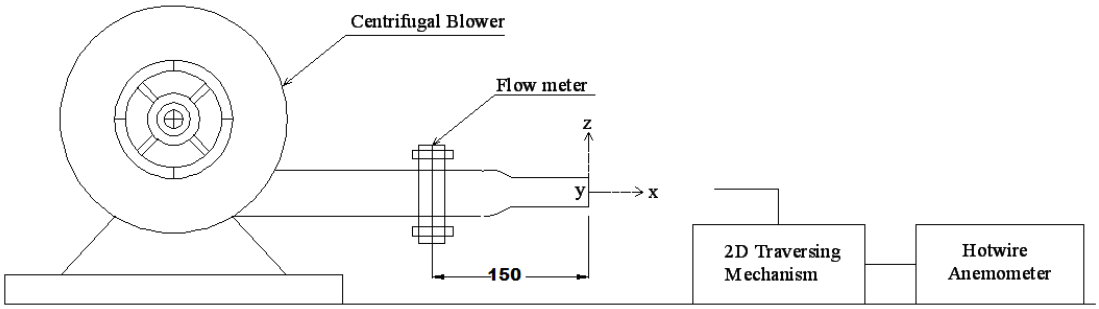

Figure 1 Experimental setup

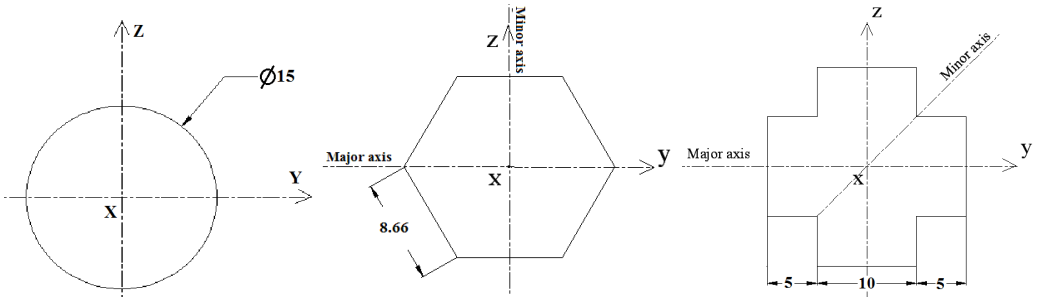

[a] [b] [c]

Figure 2 Jet shapes

A single hotwire probe was used to measure the velocity at the exit of the pipe and along the centerline of the air jet. The probe was a 5 micron diameter tungsten wire with a sensing length of 0.4 mm. It was controlled by Dantec streamline-90N10 [CTA module-90c10] anemometer, interfaced with stremware software, which is incorporated voltage gain and off-set capabilities for optimizing the analog output for the voltage range of the 12 bit analog to digital converter. Calibration of the hotwire was performed with the position (X/D_h = 1) in the potential core region of the circular jet over a velocity range of 12-45 m/s. The calibration data was fitted to a general king's law relation. $E^2 = A + BU^n$, Where E is the hotwire voltage output, and A, B and n are calibration constants, assume n = 0.45, this is common for hot-wire probes. A and B can be found by measuring the voltage E, obtained for a number of known flow velocities and performing a least squares fit for the values of A

and B which produce the best fit to the data. By defining U^n = x and E^2 = y, this least squares fit becomes simply a linear regression for y as a function of x. The values of A and B are 5.98 and 4.608. It depend on the settings of the anemometer circuitry, the resistance of the wire using, the air temperature, and to a lesser extent the relative humidity of the air. Note that the uncertainty in the determination of the mean flow velocities [which are obtained from the Pitot - static tube] implies an uncertainty in the calibration and thus in the velocities obtained from the hot-wire probe.

3. Exit Conditions

The three studied air jets are generated from a circle, hexagon and cruciform nozzles having a same hydraulic diameter D_h =15 mm based on the exit area A and perimeter P, D_h = (4A/P) (fig. 2). The exit profiles of the streamwise velocity, measured at X/D_h = 0 are represented in fig. 3 (a),(b) & (c). The initial Reynolds number is based on the centerline exit velocity and on the hydraulic diameter for all the three jets. The magnitude of the centerline mean velocity of asymmetric jet was less than the axisymmetric jets. The corners and flat sides of the asymmetric jets produce the vortices, due to that the magnitudes of the centerline mean velocity was reduced. When you compare with the circular jet, hexagon jet has 11.96% and cruciform jet has 12.75% lesser. This will show the effect of the nozzle geometry.

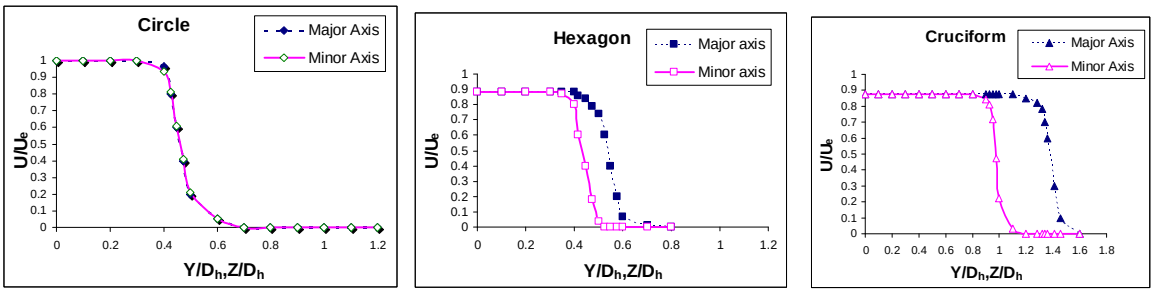

[a] **[b]** **[c]**

Figure 3 Exit conditions [a] Circular jet. [b] Hexagon jet [c] Cruciform jet

Figure 4 presents the centerline mean velocity profiles at a near-field region, i.e. X/D_h = 1 (which corresponds to the first streamwise location measured), for the three different nozzles tested in the present study. For the various nozzle, the mean velocity profiles and their corresponding fluctuating components are presented only for the major plane [X − Y].

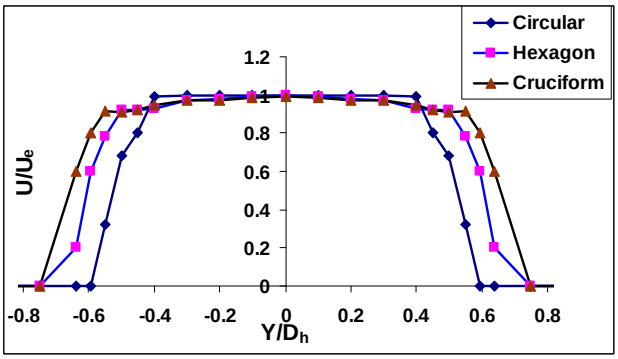

Figure 4 Velocity profiles along the streamwise direction for various nozzle geometries at X/D_h=1.

Figure 5 shows the corresponding turbulence intensities at X/D_h = 1. At this location, u'/U_{cl} varies significantly from 4% at Y/D_h = 0 to 19% at the jet edge for the circular, while for the other

nozzles u'/U_{cl} spans between 1.9% and 23%. The asymmetric nozzles have the highest shear layer turbulence intensities at this location.

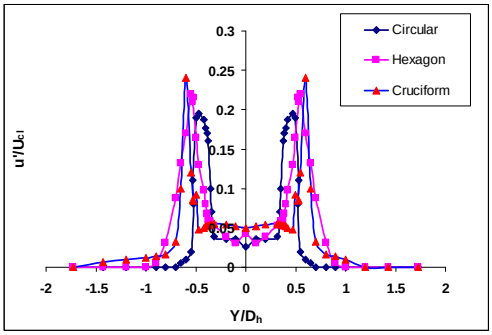

Figure 5 Radial profiles of the mean fluctuating velocity components for various nozzle geometries. (X/D_h =1)

4. Results and Discussions

4.1 Properties along the direction of jet axis

4.1.1 Potential core length

The potential core is where the flow characteristics match those of the nozzle-exit. The potential core length of circular, hexagon and cruciform jets was 4.25D_h, 3.5D_h & 2.9D_h respectively. The variation of the core length of various jets was shown in fig. 6. The non-circular jets have shorter potential core length compared to the circular jet. It is due to the effect of the nozzle shapes having corners and flat sides. When comparing these shapes with circular jet, the reduction of core length in the case of hexagon jet was 17.6% and cruciform jet was 31.7%. Within the noncircular shapes, the cruciform jet core length was shorter because the numbers of corners are more than the hexagonal shape. Coherent structures could be generated at the flat sections of nozzle. But the corner flow was predominantly three dimensional with small scale turbulence. The amplification rate of the turbulence fluctuations was higher for at the flat side due to the higher vorticity content.

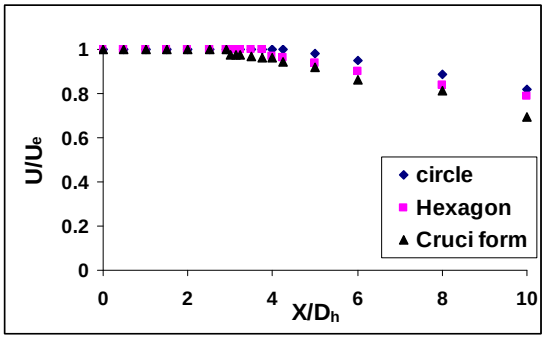

Figure 6 Comparison of Potential core length of different jets

4.1.2 Mean streamwise centerline velocity Field

It is well known that the mean velocity decay can be divided into three regions, an initial region, a characteristic region and axisymmetric decay region as shown in fig.7.

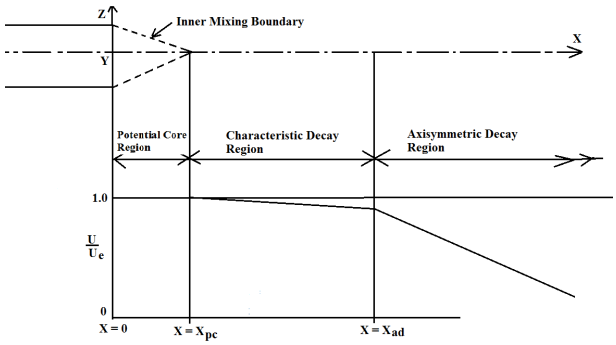

Figure 7 Schematic representation of flow field of free jet

The initial region, here the mixing initiated at the jet boundaries has not yet permeated the entire flow field, thus leaving a region that is characterized by a constant axis velocity close to the exit velocity. It is characterised by a uniform velocity on the axis, the length of the potential core is X_{pc}. As can be seen Fig. 7, the length of the initial region depends strongly on the initial geometry of the jet. When a jet issues from an orifice, X_{pc} is much longer due to the separation from the internal edge of the nozzle followed by acceleration of the jet. A comparison of jets with the number of sides shows that X_{pc} decreases with increasing the number of sides/corners. This region depends upon the minor axis dimension of the nozzles.

In the characteristic decay region, herein the axis velocity decay is dependent upon orifice configuration, and velocity profiles in the plane of the minor axis are found to be similar, whereas those in the plane of the major axis are non similar. Hence, this region is termed “characteristic” of the initial geometry. The length of the region $X_{ad,}$ the velocity decays proportional to x^n. This region depends upon the major axis dimension of the nozzles. The exponent n is generally a function of aspect ratio of the nozzle geometry. The aspect ratio of the nozzle approaches to unity the characteristic region degenerates into a transition region between the potential core and axisymmetric decay regions.

In the axisymmetric decay region, the axis velocity decay in this region is axisymmetry in nature, ie., the axial velocity decay is proportional to x^{-1}, the entire flow is found to approach axisymmetry, thus becoming independent of the orifice geometry. Profiles in both symmetry planes in this region are found to be similar.

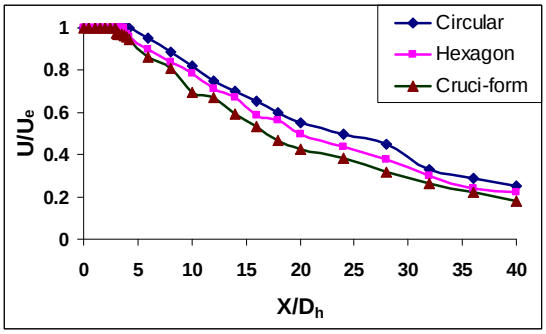

Figure 8 Comparison of centerline velocity distribution of different jets

The parameter which determine, the axial mean velocity decay of the three regions for all investigated jets are presented in tab. 1. Where, besides $X_{pc,}$ the cross point of the jet half width X_{ad} and velocity decay rate is also given. The axial velocity decay of the jets was shown in fig. 8. In the characteristic region, the decay rate of hexagonal jet was 9.1% and cruciform jet was 16.9% greater than the circular jet. It shows that the velocity decay rate of the circular jet was less than the non-circular jet.

Table 1 Details of the axial velocity regions

Nozzle	Potential core region X_{pc}	Axis switching point X_{ad} in mm	X_{ad}/D_h	Axial Velocity Decay rate
Circle (Xu & Antonia) (Ref,no,26)	$4.4D_h$	-	-	0.1511
Circle	$4.25\ D_h$	-	-	0.1464
Hexagon	$3.5\ D_h$	67.5	4.5	0.1597
Cruciform	$2.9\ D_h$	93	6.2	0.1711

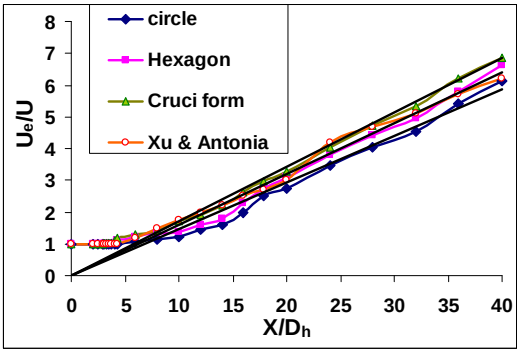

Figure 9 Comparison of reciprocal of axial velocity decay of different jets

Figure 9 shows the effect of asymmetric nozzles on the streamwise centerline mean velocity decay. For a self-preserving circular jet, the centerline mean velocity decay is expressed as [25]

$$\frac{U_e}{U_{cl}} = \frac{1}{C_1}\frac{(x-x_{01})}{D_h} \qquad (1)$$

For a circular jet, it is usually assumed that the self preserving region is at $X/D_h \geq 20$ [1, 2, 16, 18, 19, 26]. Consequently, the eq. (1) is used to fit the measured data presented in fig.9 in the range between X/D_h = 20 to 40, where for the circular nozzle, C_1 and x_{01} are found to be approximately 5.91 and 3.68 D_h, respectively. The present value of C_1 is good agreement with published values reported in tab. 2 except Iyogun and Birouk [3], however, the present x_{01} seem to be in not good agreement with that of Iyogun and Birouk, [3]. One may attribute this discrepancy in C_1 to the difference in the exit conditions of the circular's jet [e.g., Reynolds number, orifice exit shape] or the technique employed by the different investigators to measure the jet velocity profiles. Nevertheless, the published velocity measurements were obtained by using Laser Doppler anemometer

(LDA) [1, 4, 26,] whereas hot-wire anemometry is used in the present study. It has been found that measurements of mean velocities and their fluctuating components obtained using hot-wire anemometry exhibit some differences compared to those obtained by using Laser Doppler Velocimetry [LDV]. However, since the value of C_1 reported by Capp et al.[2] is nearly similar to published results of Boersma et al.[1] and Rodi. [19]

Table 2 Jet Decay rate for the circular nozzle.

Sl. No	Reference	U m/s	Measurement Technique	D_h (mm)	Re x 10-3	C_1	X_{01}
1	Present work	15	Hot-wire	15	15.4	5.91	3.68 D_h
2	Christopher O. et. al	30	LDV	4.82	9.4	6.23	1.45 D_h
3	Xu and Antonia	23.3	Hot-wires	55	86	5.6	3.7 D_h
4	Borsema et al.		DNS		2.4	5.9	
5	Capp et al.	56.2	LDA	25.0	95.5	5.8	2.7 D_h
6	Capp et al.	56.2	Hot-wires	25.0	95.5	5.9	2.7 D_h
7.	Rodi	101	Hot-wire	12	87	5.9	
8	Panchapakesan & Lumley	27	Hot-wire	6.1	11	6.06	-2.5 D_h

In fact, the value of C_1 for a circular nozzle obtained, with the same test conditions, by using hot-wire anemometry and LDV was quite different Hussein et.al. [11]. some of these discrepancies were assumed to be caused by the cross-flow and rectification errors present in stationary hot-wire measurements. However, even the flying hot-wire measurements were also found to differ from those acquired by using LDV Hussein et.al. [11]. Therefore, the reason for the discrepancy in the values of C_1 between the present study and published studies may be attributed to the different techniques used for velocity measurement.

Using eq. (1) and the same X/D_h range reported above for the corresponding values for the circular, hexagon and cruciform jets are C_1 = 5.91, 5.62, & 5.51 while x_{01} is 3.68 D_h, 2.71 D_h and 2.25 D_h respectively [see tab. 3]. The linear fit for all nozzle jets have almost perfect value of R^2 which is around 1. This value corresponds to a good fit. It has to be acknowledged that using the same self-similar region for computing C_1 and x_{01} does not in any way imply that all nozzles achieve self-similarity at the same streamwise location. The present measured value of C_1 for the circular jet is in good agreement with most published data, as shown in tab. 2 though it is not close to the value of 6.23 & 6.06 obtained by Iyogun and Birouk [3] and Panchapakesan and Lumley [16] respectively.

Table 3 Jet Decay rate for different nozzle's geometries

Sl.No	Geometries	C_1	X_{01}
1	Circle	5.91	3.68 D_h
2	Hexagon	5.62	2.71 D_h
3	Cruciform	5.51	2.25 D_h

The value of x_{01} for the present circular jet is also not in agreement with the values reported in tab. 2 except Xu and Antonia [26]. These discrepancies may be partly caused by the same reasons as for C_1. However, the value of x_{01} can be different for different shapes of the nozzles. In fact, it has been shown that an increase in the number sides can lead to a increase in the rate of jet entrainment as a result of an increase in the streamwise mean velocity decay, which in turn engenders an decrease in the potential core of the jet (i.e. a decrease in x_{01}) by Warda et.al. [24]. Figure 9 shows clearly that with a jet bulk exit velocity of 15 m/s, the jet decay is faster for the cruciform nozzle, followed by the hexagon, with the circle has the lowest. This trend confirms the findings reported by Mi et al. [13] amongst others. This is more evident when observing the centerline streamwise mean-velocity decay of the jet's near-field region [i.e. $X/D_h \leq 15$], as shown in fig. 9.

What can be retained from the brief discussion above and from fig. 9 is that the coefficient C_1 seems capable of predicting the trend of the velocity decay rate for all nozzles geometries. It appears that the mean velocity decays more rapidly when lower the value of C_1 by Xu and Antonia [26]. Also the values of x_{01} reflect the trend of rate jet entrainment. It has been shown that the lower the x_{01}, the higher the rate of entrainment by Wygnanski and Fieldler [25].

However, if C_1 and x_{01} of each individual nozzle, as presented in tab. 2 and tab. 3, are combined then they can predict an overall pattern or the velocity decay rate and entrainment rate of the tested nozzles. Moreover, C_1 and x_{01} are sufficient to predict the nozzles' streamwise mean velocity decay in the far-stream.

4.1.3 Turbulence intensities

The turbulence intensity is defined as the velocity fluctuation root-mean square scaled to the local mean velocity. Figure 10 displays a plot of the centerline turbulence intensity in the three regions of all the test cases examined.

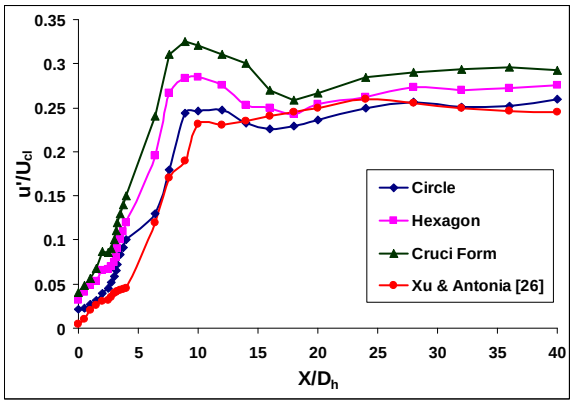

Figure 10 Variations of Turbulence intensities along the jet axis.

1) In the region of jet flow establishment, this quantity features a peculiar behaviour. Indeed, a sudden rise is present from $X/D_h = 1$ leading to a peak whose position shows a slight Reynolds dependence, and rises to a global maximum in the surroundings of $X/D_h = 8$. For the investigated jets the turbulence intensity increases strongly in the initial region as the result of the free mixing layer formed by the initial instability. Downstream a toroidal vortex structure is generated due to the momentum transfer from the central region to the surrounding mixing layer; actually the instability

wave develops into such a vortex structure. Later on this structure breaks down and a maximum of the turbulence intensity will be reached.

The maximum turbulence intensity and its location X_{max} depend on the initial conditions as can be seen in fig. 10. At the same time no clear regularity in this dependence is observed, except for the jet with circular cross section. This increase is faster for cruciform shape jet, an explanation of this fact could be the more intensive interaction between the longer sides of cruciform vortex frame close to the exit.

2) In the characteristic decay region of the jet, Turbulence intensity tends to a constant level of about 0.26. This was close to values reported recently in Gutmark et.al. [7]. However, this value is not reached in all the jets tested. In the flow out of sharp-edged nozzles, particularly the cruciform ones, turbulence intensity reaches a maximum of 0.325. Also, in these jets the turbulence level does not stabilize at a constant value for any appreciable length. It decreases rapidly before starting to increase again as we approach the axisymmetric-flow region.

3) In the axisymmetric region, and where measurements were taken at large distances from the exit, turbulence intensity seems to stabilize at a level close to 0.275. The dip which occurs in the region of transition from two dimensional to axisymmetry is more pronounced for jets out of sharp nozzles. It is barely noticeable for the other jets.

4.2 Mean Velocity along the cross sections of the jets.

Figure 11 shows the mean velocity profiles at X/D_h = 5. This figure clearly shows the departure from the nearly top-hat velocity profile shape that is seen at X/D_h = 1. This is an indication of the entrainment of the ambient fluid that has already taken place up to this flow location. Furthermore, this figure shows that the U/U_e profile for the noncircular nozzles is wider than that of the circular counterparts as a result of the higher spreading and entrainment of the noncircular nozzles. Figure 12 shows the radial distribution of u'/U_{cl} for the different nozzles tested here. This figure demonstrates that the noncircular nozzles have higher turbulence intensities at the nozzle edges compared to their circular counterparts. However, the cruciform jet seems to have a relatively flatter center compared to all other nozzles which is also a characteristic of the mean streamwise velocity distribution at this location, as shown in fig.11.

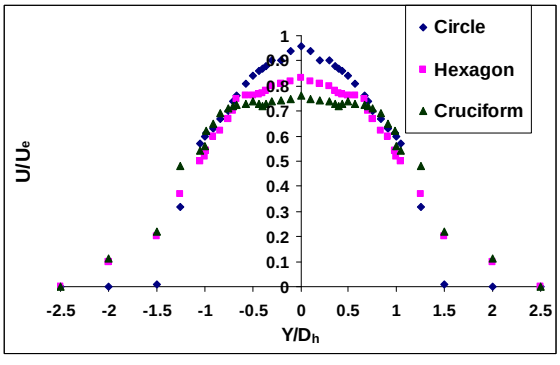

Figure 11 Radial profiles of the mean velocity components for various nozzle geometries at X/D_h =5

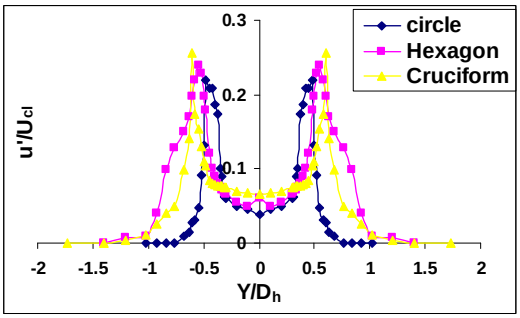

Fig.12 Radial profiles of the fluctuating velocity components for various nozzle geometries at $X/D_h = 5$.

This flatness of the turbulence intensity profile in the center of the cruciform jet is an indication that the turbulence intensities are concentrated at the edges of the noncircular nozzles though not very obvious for the hexagonal nozzle because of the plane of measurement used and the configuration of the geometry. Consequently, this figure emphasizes again the influence of asymmetric nozzles on the rate of ambient air entrainment since the mean centerline velocity decay correlates well with the radial distributions of u'/ U_{cl} at the nozzle edges.

Figures 13 [a] & [b] show the radial distribution of the normalized mean velocity profiles at X/D_h = 10 and 20, respectively, The location X/D_h = 20 is chosen because it is assumed that downstream of this normalized streamwise location, the mean velocity profiles of an axisymmetric jet becomes self-similar. Furthermore, the effect of noncircular is clearly evident from these figures. The profile of the noncircular configuration is seen to be wider than the circular configuration indicating a greater jet's spreading rate of the noncircular configuration compared to the circular configuration.

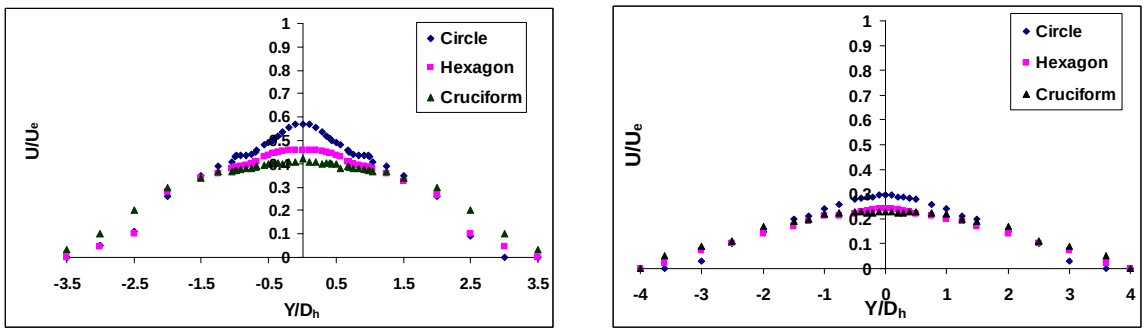

[a] **[b]**

Figure 13 Radial profiles of the streamwise mean-velocity for various nozzle geometries. [a] X/D_h =10, [b] X/D_h =20.

Figures 14 [a] & [b] show the radial distribution of u'/U_{cl} at X/D_h = 10 and 20, respectively, for the different nozzles tested here. Again, it is clearly shown in these figures that the turbulence intensity profiles of the noncircular configurations are wider and much larger than the circular configurations. This also confirms the initial stipulation that the rate of entrainment and spreading correlates well with the increase in turbulence intensities at the edges. Mixing is initiated at the edges or corners and the higher the turbulence at these edges and corners, the higher the entrainment and spreading rates. Consequently, the asymmetric nozzles, which have the highest turbulence intensities at the edges, have also higher jet entrainment and spreading compared to their circular counterparts.

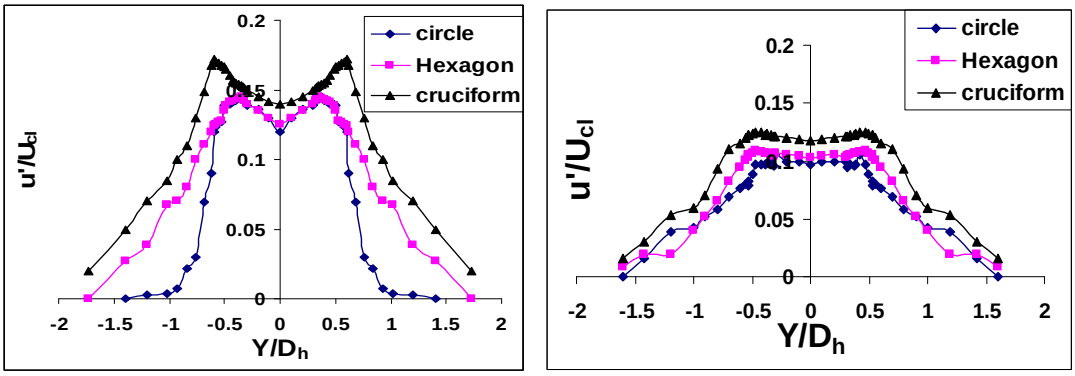

[a] **[b]**

Figure 14 Radial profiles of the fluctuating velocity components for various nozzle geometries [a] X/D_h =10, [b] X/D_h = 20.

In addition, fig. 14[b] which shows the profile of u'/U_{cl} at X/D_h = 20 gives the impression that the profiles of the mean fluctuating components have not reached self-similarity at this location. This is in accordance with the proposition by Boersma et al. [1] that self-similarity for the velocity fluctuations can only occur at X/D_h > 35 for axisymmetric nozzles.

4.3 Development of the jet half-velocity width

Figure 15 presents the jet spreading as a function of X/D_h along the major plane [X − Y] of the various nozzles as the planes shown in fig.2. The jet boundary was determined by using the velocity profiles. The streamwise growth of the vertical transverse coordinate Y at which the mean velocity attains half of its maximum value has been useful as a correlation factor in mixing problems. The noncircular jet half width was more than the circular jet. From the trend, near the inlet the jet half-width of a cruciform jet is higher than the all jets and far away a location when compare with the circular jet, the increase of half width in the case of hexagon jet was 4% and cruciform jet was 36%. Within the noncircular shapes, the cruciform jet half width was 28% more than the hexagonal jet.

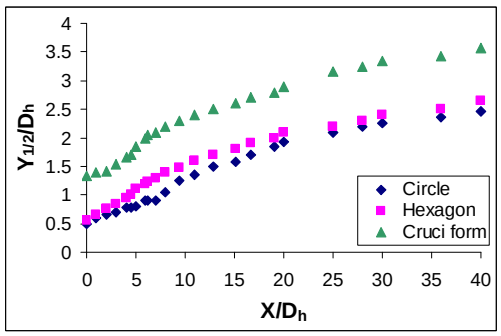

Figure 15 Comparison jet half widths of three jets

The requirement for self-preservation for a round jet, according to Xu and Antonia [26], is given as

$$\frac{Y_{1/2}}{D_h} = C_2 \frac{(x-x_{02})}{D_h} \quad (2)$$

However, the maximum streamwise location where the jet spread is measured for each nozzle is at $X/D_h = 30$ and therefore only two locations (i.e. $X/D_h = 20$ and 30) are used to compute C_2 and x_{02}. The experimental data for each nozzle's geometry, which is presented in fig. 17, is used to fit eq. (2). The values of C_2 and x_{02} are found to be 0.095 and $-1.81D_h$; 0.097 and $-1.34D_h$; 0.098 and $-1.27\ D_h$; for the circular, hexagon and cruciform jet, respectively. The present value of C_2 for the circular jet is in good agreement with the LDA measurements of Capp et al. [2], the hot-wire measurement of Xu and Antonia [26], and the hot-wire measurements of Panchapakesan and Lumley [16] who obtained a value of C_2 equal to 0.094, 0.095 and 0.096, respectively, as shown in tab. 4. However, the present value of C_2 is in not good agreement with those of Rodi [19] and Wygnanski and Fieldler [25] who both obtained a value of 0.086. These differences may, in part, be due to the variation of the nozzle's orifice contraction profile used by each investigator, and also possibly in part to the different measurement techniques employed. It has to be emphasized that the values of C_2 and x_{02} when used individually do not give a very clear indication of the trend of the spreading rate when comparing between different nozzles especially the asymmetric nozzles. For example, the near-field of the hexagonal and cruciform nozzle gives the impression that they have higher rate of spread; however, the far-field shows that the circular nozzle become higher. This discrepancy is due to the fact that the circular nozzle, and to some extent the hexagon and cruciform nozzle have symmetric mean velocity profiles across most of the planes.

Table 4. Jet spreading rate for the circular nozzle.

Sl.No	Reference	C_2	X_{02}
1	Present work	0.092	-1.81 D_h
2	Christopher O. et.al.	0.085	-1.78 D_h
3	Capp et al.	0.094	-
4	Panchapakesan & Lumley	0.096	-
5	Xu and Antonia	0.095	-
6	Wygnanski and Fieldler	0.086	-
7.	Rodi	0.086	-

Table 5 Jet spreading rate for different nozzles geometries

Sl.No	Geometries	C_2	X_{02}
1	Circle	0.092	-1.81 D_h
2	Hexagon	0.089	-1.34 D_h
3	Cruciform	0.082	-1.27 D_h

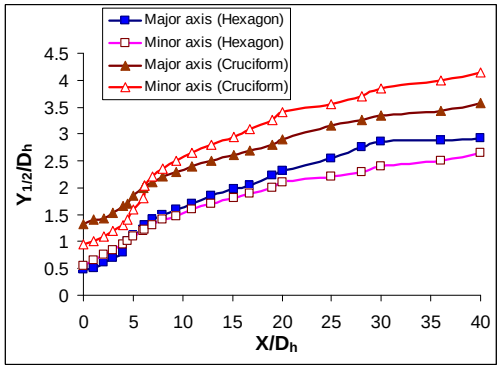

Figure 16 Jet half width variations along the major and minor axis of hexagon and cruciform jet

The fig.16 shows the well known difference in spreading rate of the jet in the two directions. The crossing point of the two curves for the XOY, XOZ planes, respectively, marks the domain where the axial velocity decay becomes proportional to X^{-1}. Obviously, this is not yet the fully developed region of the jet which appears too far from the exit cross section. These results indicate that for three dimensional jets the major axis half width decreases initially, whereas the minor axis half width grow similarly but at different rates, and finally tend to axisymmetry. This phenomenon is termed as axis switching and it has been shown that as its frequency of occurrence increases, the rate of entrainment and subsequently mixing is increased. It is interesting to note that in this case the cross over point corresponds to the onset of axisymmetric decay. Figure 18 shows that the half width variation of a hexagon and cruciform jet along the minor and major axis planes respectively. From the trend that the half-width variation in the two orthogonal planes, it is recognized that the hexagonal jet axis switching takes place at a distance of $X/D_h = 4.5$ and cruciform jet flow case axis switching is seen to occur at a distance of $X/D_h = 6.2$. In hexagonal case, at the far field the jet half-width in the major axis was 15.5% less than the minor axis. In the cruciform shape the jet half-width of major axis was 23% less than the minor axis.

5. Conclusion

In this study, the single hotwire measurements were carried out for the three single jets issuing respectively from circular, hexagonal and cruciform nozzles with same operating conditions. Comparison has been made between the near-field mixing characteristics of the jets. It has been found that, in general, the circular jet has more potential core and less velocity decay and jet half width when compared to the non circular jets. In the noncircular shapes the cruciform jet entrains the ambient fluid at a higher rate than the circular counterpart. Specifically, the hexagonal and cruciform jets decays and spreads faster, yielding a shorter potential core. Immediate downstream from the nozzle exit [$X < 3.5D_h$], mixes the surroundings much faster and the phenomenon of axis switching occurs at $X = 4.5D_h$ for hexagonal jet and $X = 6.5D_h$ for cruciform jet. The coefficient C_1 seems capable of predicting the trend of the velocity decay rate for all nozzles geometries. It appears that the mean velocity decays more rapidly when lower the value of C_1. Also the values of x_{01} reflect the trend of rate jet entrainment. It has been shown that the lower the x_{01}, the higher the rate of entrainment. Comparing the profiles of the turbulence intensity and the profiles of the mean velocity, it can be

concluded that the turbulence intensity profiles have a maximum at the location where the velocity has a maximum gradient.

6. Nomenclature

A - Area of the nozzle. [m^2]
C_1, C_2 - Decay constant
D - Diameter of the nozzle. [m]
D_h - Hydraulic diameter of the nozzle. [m]
P - Perimeter of the nozzle. [m]
Re - Reynolds Number (=UD/ ν)
U - Velocity of the jet at streamwise direction. [m/s]
U_{cl} - Velocity of the jet along the centerline. [m/s]
U_e - Velocity of the jet at the exit. [m/s]
x_{01} - Kinematic virtual origin [m]
x_{02} – Geometric virtual origin [m]
X_{pc} – Length of the Potential core region [m]
X_{ad} – Length of the characteristic region [m]
X - Axial coordinate in the flow direction. [m]
$Y_{1/2}$ - Jet half-velocity width, [m]
Y, Z - Coordinates in the lateral direction. [m]
ν - Kinematic viscosity of the fluid. [m^2/s]

7. Reference

[1]. Boersma, B.J., Brethouwer, G., Nieuwstadt, F.T.M., A Numerical Investigation on the Effect of the Inflow Conditions on the Self-similar Region of a Round Jet, *Physics of Fluids,10* [1998], pp. 899–909.

[2]. Capp, S.P., Hussein, H.J., George, W.K., Velocity Measurements in a High Reynolds Number Momentum-conserving, Axisymmetric, Turbulent Jets, Technical Report. 123. Turbulence Research Laboratory, University at Buffalo, Suny [1990].

[3]. Christopher, O. Iyogun., and Madjid Birouk., Effect of Sudden Expansion on Entrainment and Spreading Rates of a Jet Issuing from Asymmetric Nozzles, *Journal of Flow Turbulence Combustion, 82* [2008], 3, pp. 287-315.

[4]. Ferdman, E., Otugen, M.V., Kim, S., Effect of Initial Velocity Profile on the Development of Round jets, *Journal of Propulsion Power, 16* [2000], pp. 676–686.

[5]. Grinstein, F.F., Self-induced Vortex Ring Dynamics in Subsonic Rectangular Jets, *Physics of Fluids, 7* [1995], pp. 2519-2521.

[6]. Grinstein, F.F., Gutmark, E., Parr, T., Near Field Dynamics of Subsonic Free Square Jets, A Computational and Experimental Study, *Physics of Fluids, 7* [1995], pp. 1483-1497.

[7]. Gutmark, E., Grinstein, F.F., Flow Control with Noncircular Jets, *Annual Review of Fluid Mechanics, 31* [1999], pp. 239-272.

[8]. Gutmark, E., Schadow, K.C., Parr, T.P., Hanson-Parr, D.M., Wilson, K.J., Noncircular Jets in Combustion Systems, *Experiments in Fluids, 7* [1989], pp. 248-258.
[9]. Gutmark, E., Schadow, K.C., Wilson, K.J., Subsonic and Supersonic Combustion Using Noncircular Injectors, *Journal of Propulsion Power, 27* [1991], pp. 240–249.
[10]. Ho, C., Gutmark, E., Vortex Induction and Mass Entrainment in a Small-aspect-ratio Elliptic Jet, *Journal of Fluid Mechanics, 179* [1987], pp. 383–405.
[11]. Hussein, H.J., Capp, S.P., George, W.K., Velocity Measurements in a High-Reynolds-number, Momentum-Conserving, Axisymmetric, Turbulent Jet, *Journal of Fluid Mechanics, 258* [1994], pp. 31–75.
[12]. Koshigoe, S., Gutmark, E., Shadow, K., Initial Development of Non-circular Jet Leading to Axis Switching, *AAIA Journal, 27* [1989], pp. 439.
[13]. Mi,J., Nathan,G.J., Luxton,R.E., Centerline Mixing Characteristics of Jets from Nine Differently Shaped Nozzles, *Experiments in Fluids, 28* [2000], pp. 93-94.
[14]. Mi, J., Nathan, G.J., Nobes, D.S., Mixing Characteristics of Axisymmetric Free Jets from a Contoured Nozzle, an Orifice Plate and a Pipe, *Journal of Fluids Engineering, 123* [2001], pp. 878–883.
[15]. Miler, R.S., Madnia, C.K., Givi.P., Numerical Simulations of Non-circular Jets, *Journal of Computers & Fluids, 24* [1995], pp. 1-25.
[16]. Panchapakesan, N.R., Lumley, J.L., Turbulence Measurements in Axisymmetric Jets of Air and Helium. 1. Air jet, *Journal of Fluid Mechanics, 246* [1993], pp. 197–223.
[17]. Quinn, W.R., On Mixing in an Elliptic Turbulent Free Jet, *Physics of Fluids A 1* [1989], pp. 1716–1722.
[18]. Quinn, W.R., Measurements in the Near Flow Field of an Isosceles Triangular Free Jet, *Experiments of Fluids, 39* [2005], pp. 111–126.
[19]. Rodi, W., A New Method of Analyzing Hot-wire Signals in Highly Turbulent Flow and its Evaluation in a Round Jet, DISA Inf. 17, [1975, Feb]
[20]. Sau, A., Vortex Dynamics and Mass Entrainment in a Rectangular Channel with a Suddenly Expanded and Contracted Part, *Physics of Fluids, 14* [2002], pp. 3280–3308.
[21]. Sau, A., Generation of Streamwise Vortices in Square Sudden-expansion Flows, *Physics Review. E 69* [056304] [2004], pp. 1–10.
[22]. Shigetaka Fujita., Hideo Osaka., Effect of Aspect Ratios on Potential Core Length for Cruciform Jet, *Experimental Thermal and Fluid Science, 5* [1992], pp. 332-337.
[23]. Vagt, J.D., Hotwire Probes in Low Speed Flow, *Prog. Aerospace Science, 18* [1979], pp. 271-323.
[24]. Warda, H.A., Kassab, S.Z., Elshorbagy, K.A., Elsaadawy, E.A., An Experimental Investigation of the Near-field Region of Free Turbulent Round Central and Annular Jet, *Journal of Flow Measurement and Instrumentation, 10* [1999], pp. 1–14.
[25]. Wygnanski, I., Fiedler, H., Some Measurements in the Self-preserving Jets, *Journal of Fluid Mechanics, 38* [1969], pp. 577–612.
[26]. Xu, G., Antonia, R.A., Effect of Different Initial Conditions on a Turbulent Round Free Jet, *Experiments of Fluids, 33* [2002], pp. 677–683.
[27]. Zaman, K.B.M.Q., Spreading Characteristics of Compressible Jets from Nozzles of Various Geometries, *Journal of Fluid mechanics, 383* [1999], pp. 197-228.

[28]. Zaman, K.B.M.Q., Axis Switching and Spreading of an Asymmetric Jet: the Role of Coherent Structure Dynamics, *Journal of Fluid Mechanics, 316* [1996], pp. 1–27.